Suppression of HER2/HER3-Mediated Growth of Breast Cancer Cells with Combinations of GDC-0941 PI3K Inhibitor, Trastuzumab, and Pertuzumab

Evelyn Yao, Wei Zhou, Si Tuen Lee-Hoeflich, et al.

Clin Cancer Res 2009;15:4147-4156.

Suppression of HER2/HER3-Mediated Growth of Breast Cancer Cells with Combinations of GDC-0941 PI3K Inhibitor, Trastuzumab, and Pertuzumab

Evelyn Yao,[1] Wei Zhou,[1] Si Tuen Lee-Hoeflich,[2] Tom Truong,[1] Peter M. Haverty,[3] Jeffrey Eastham-Anderson,[2] Nicholas Lewin-Koh,[4] Bert Gunter,[4] Marcia Belvin,[1] Lesley J. Murray,[1] Lori S. Friedman,[1] Mark X. Sliwkowski,[1] and Klaus P. Hoeflich[1]

Abstract

Purpose: Oncogenic activation of the phosphatidylinositol 3-kinase (PI3K) signaling pathway is prevalent in breast cancer and has been associated with resistance to HER2 inhibitors in the clinic. We therefore investigated the combinatorial activity of GDC-0941, a novel class I PI3K inhibitor, with standard-of-care therapies for HER2-amplified breast cancer.

Experimental Design: Three-dimensional laminin-rich extracellular matrix cultures of human breast cancer cells were utilized to provide a physiologically relevant approach to analyze the efficacy and molecular mechanism of combination therapies *ex vivo*. Combination studies were done using GDC-0941 with trastuzumab (Herceptin), pertuzumab, lapatinib (Tykerb), and docetaxel, the principal therapeutic agents that are either approved or being evaluated for treatment of early HER2-positive breast cancer.

Results: Significant GDC-0941 activity (EC_{50} <1 μmol/L) was observed for >70% of breast cancer cell lines that were examined in three-dimensional laminin-rich extracellular matrix culture. Differential responsiveness to GDC-0941 as a single agent was observed for luminal breast cancer cells upon stimulation with the HER3 ligand, heregulin. Combined treatment of GDC-0941, trastuzumab, and pertuzumab resulted in growth inhibition, altered acinar morphology, and suppression of AKT mitogen-activated protein kinase (MAPK) / extracellular signed-regulated kinase (ERK) kinase and MEK effector signaling pathways for HER2-amplified cells in both normal and heregulin-supplemented media. The GDC-0941 and lapatinib combination further showed that inhibition of HER2 activity was essential for maximum combinatorial efficacy. PI3K inhibition also rendered HER2-amplified BT-474M1 cells and tumor xenografts more sensitive to docetaxel.

Conclusions: GDC-0941 is efficacious in preclinical models of breast cancer. The addition of GDC-0941 to HER2-directed treatment could augment clinical benefit in breast cancer patients.

Phosphatidylinositol 3-kinase (PI3K) was first identified as an enzymatic activity associated with viral oncoproteins that phosphorylated phosphatidylinositol at the 3′-hydroxyl of the inositol ring (1). The PI3K family comprises 15 different enzymes that are divided into three classes based on their substrate preference and sequence homology (2). Class I PI3K consists of the PIK3CA, PIK3CB, PIK3CD, and PIK3CG isoforms. These kinases are involved in signal transduction events downstream of cytokines, integrins, and growth factors, and have been implicated in cellular responses relevant to tumorigenesis, including cell proliferation, motility, survival, and angiogenesis. Oncogenic mutations of *PIK3CA* have been found to occur at significant frequency in colon, breast, brain, liver, ovarian, gastric, lung, and head and neck solid tumors (3, 4). Moreover, inactivation of PTEN, a tumor suppressor and negative regulator of PI3K signaling, occurs in numerous tumor types and results in a constitutive up-regulation of class I PI3K activity (5). These recent discoveries have heightened the interest in developing small molecule inhibitors of PI3K isoforms and their effectors (6).

The PI3K signaling pathway is also of central importance in HER2-amplified breast cancer (7). HER2 homodimers and heterodimers have been shown to activate numerous downstream signaling events, including PI3K activation (8–10). In particular, upon heregulin stimulation the HER2/HER3 signaling complex potently activates the PI3K pathway by directly coupling to the p85 regulatory subunit of PI3K (11). Dysregulation of the HER3-PI3K axis has been implicated as a resistance mechanism to HER2-targeted therapies, such as

Authors' Affiliations: Departments of [1]Cancer Signaling and Translational Oncology, [2]Pathology, [3]Bioinformatics, and [4]Biostatistics, Genentech, Inc., South San Francisco, California

Received 10/28/08; revised 3/4/09; accepted 3/16/09; published OnlineFirst 6/9/09.

The costs of publication of this article were defrayed in part by the payment of page charges. This article must therefore be hereby marked *advertisement* in accordance with 18 U.S.C. Section 1734 solely to indicate this fact.

Note: Supplementary data for this article are available at Clinical Cancer Research Online (http://clincancerres.aacrjournals.org/).

Requests for reprints: Klaus P. Hoeflich, Genentech MS 50, 1 DNA Way, South San Francisco, CA 94080. Phone: 650-225-6697; Fax: 650-225-5770; E-mail: hoeflich@gene.com.

doi:10.1158/1078-0432.CCR-08-2814

Translational Relevance

The development of pharmacologic agents to target PI3K isoforms or their effector kinases is an area of intense investigation. In this article, we describe the biological effects of GDC-0941, a small molecule inhibitor of class I PI3-kinases that is currently being evaluated in human clinical trials for the treatment of cancer. We show that GDC-0941 acts in concert with trastuzumab (Herceptin), pertuzumab, and lapatinib (Tykerb) to dramatically decrease the growth and morphogenesis of breast cancer cells. The importance of these results is underscored by recent evidence suggesting that dysregulation of the PI3K signaling pathway is a mechanism of therapeutic resistance to HER2-targeted therapies. In this way, these preclinical studies add to our understanding of the molecular determinants for antitumor efficacy resulting from HER2/HER3 and PI3K pathway inhibition and have strong implications for therapeutic intervention in the clinic.

trastuzumab (Herceptin). For instance, exogenous ligands of HER3 have been shown to rescue cells from the antiproliferative effect of trastuzumab *in vitro* (12), and PIK3CA-activating mutations and loss of PTEN expression have been associated with poor prognosis while on trastuzumab therapy (13, 14). These findings suggest an opportunity to develop combinatorial strategies using clinical inhibitors of the HER2, HER3, and PI3K signaling networks for the treatment of breast cancer.

In glandular tissues such as the breast, the interaction between the epithelium and surrounding basement membrane (a specialized form of extracellular matrix) is critical in both maintenance of normal tissue architecture and tumor development (15–17). As such, adaptation of reconstituted, laminin-rich extracellular matrix (lrECM) to standard cell culture is an improved *in vitro* model to simulate the dynamic microenvironment of a tumor (18). We have previously employed these physiologically relevant, three-dimensional lrECM (3D lrECM) assays to account for the role of these matrix macromolecules in HER2/HER3 signaling (8). Here we utilize three-dimensional culture models of breast cancer to investigate the biological effect of GDC-0941, a selective inhibitor of class I PI3K with promising pharmaceutical properties, in HER2-amplified breast cancer cells (19). Distinct acinar phenotypes were associated with combinations of GDC-0941 and the HER2-specific antibodies, trastuzumab and pertuzumab (20, 21), and provide a novel approach for evaluating the molecular and cellular mechanism of action of these compounds. Taken together, our results support combination treatment with HER2 and PI3K inhibitors and the use of three-dimensional culture as a system for characterizing novel inhibitors and targets.

Materials and Methods

Three-dimensional cell culture and reagents. Cell lines were obtained from the American Type Culture Collection or Deutsche Sammlung von Mikroorganismen und Zellkulturen (Germany) and grown in either DMEM:F12 (BT-474M1, SK-RB-3) or RPMI (CAL120, EFM192A, HCC1419, HCC1954, Hs 578T, KPL-4, MCF-7, MDA-MB-175, MDA-MB-231, MDA-MB-361.1, MDA-MB-453, T-47D, ZR-75-30) supplemented with 10% fetal bovine serum. All cells were initially propagated on plastic in standard media. BT-474M1 cells are a tumorigenic subline of the BT474 breast cancer cell line and express high levels of HER2. BT-474M1 acinar growth was evaluated in high- and low-serum conditions, and media containing 10% fetal bovine serum yielded optimal viability and morphogenesis for 3D lrECM culture. Tissue culture dishes were coated with a thin layer of growth factor-reduced Matrigel (BD Biosciences) on ice and then placed in a 37°C incubator for approximately 15 min to allow for matrix polymerization. Cells were dislodged with trypsin and then resuspended in their respective growth media supplemented with 5% Matrigel. After mixing, cells, media, and drugs were added onto the precoated plates. For combination experiments, cells were treated with 20 μg/mL trastuzumab, 25 μg/mL pertuzumab, 250 nmol/L GDC-0941, and/or 200 nmol/L lapatinib (Genentech), with or without 1 nmol/L heregulin unless otherwise indicated. Bacterially expressed, epidermal growth factor–like domain of heregulin-β1 (residues 177-244) was purified in-house as previously described (22). Media were refreshed every 3 to 4 d for a total duration of 9 d. Nuclear accumulation of hypoxia inducible factor-1α vascular endothelial growth factor was quantified using a transcription factor ELISA. The concentration of secreted vascular endothelial growth factor in cell culture supernates was determined with a human vascular endothelial growth factor immunoassay (R&D Systems).

EC_{50} determination and cell viability. EC_{50} values were determined by seeding cells at a density of 2.8×10^3 cells per well on a 96-well microtiter plate. Twenty-four hours after plating, cell lines were treated with 0 to 20 μmol/L GDC-0941 and 1 nmol/L heregulin (administered 1 h thereafter). All conditions were done in triplicates. Assays were carried out for 72 h after drug addition. Cell viability was measured with Cell Titer Glo (Promega) according to the manufacturer's instructions. EC_{50} values were calculated by fitting plate values to a 4-parameter logistic model by nonlinear least squares.

Western immunoblot. Cells were washed in chilled PBS and harvested in a cold, PBS-EDTA solution [5 mmol/L EDTA, 1 mmol/L $NaVO_4$, 1.5 mmol/L NaF, protease inhibitor cocktail (EMD Biosciences), protease inhibitor (Sigma), phosphatase inhibitor cocktail I (Sigma), phosphatase inhibitor cocktail II (Sigma), PBS]. To dissolve the Matrigel, the harvested mixtures were placed on ice in 4°C and rocked gently for 1 h. Cells were then collected by centrifugation, lysed in radioimmunoprecipitation assay buffer, and sonicated. After a final spin, supernatant containing protein was collected from the samples.

Fifteen micrograms protein per well were resolved on 4% to 12% Bis-Tris NuPAGE gels, transferred onto nitrocellulose, and blocked in 2% bovine serum albumin-TTBS. Primary antibodies were diluted in 2% bovine serum albumin-TTBS buffer (20 mmol/L Tris-HCl, 500 mmol/L NaCl, 0.05% Tween-20, pH 7.5), and membranes were incubated overnight. Membranes were subsequently washed in TTBS, probed with a horseradish peroxidase–conjugated secondary, washed again, and exposed to X-ray film. Primary antibodies include pAkt-Thr308, pAkt-Ser473, Akt, pEGFR-Tyr1068, pHER2-Tyr1221/1222, pHER3-Tyr1289, pMEK-Ser217/221, MEK (Cell Signaling), pTyrosine peroxidase conjugate (EMD Biosciences), HER2 (Neomarkers), HER3 (Santa Cruz Biotechnology), and β-actin (Sigma).

Quantification of acinar size and shape. Phase-contrast images were captured with a Sony digital camera (DXC-S500) adapted to a Leica DMIL microscope on a 10× objective. Images were imported and analyzed in Metamorph version 7.5 (MDS Analytical Technologies). We empirically determined a global threshold of the gradient of pixel intensities that specifically identified colony borders, and applied that same threshold to each image. Some image filtering was done to remove noncolony artifacts, and incompletely imaged colonies along the image borders. The remaining colony borders were measured for their total pixel area and shape factor. An object's shape factor is defined as $(4\pi * \text{Area})/(\text{Perimeter}^2)$, resulting in a value from 0 to 1, where 0 is a flat line, and 1 is a perfect circle.

In vivo *tumor models.* Six- to eight-week-old female, beige nude XID mice from Harlan Sprague Dawley were used for our xenograft

studies. Four days prior to tumor cell inoculation, the animals were implanted with a 0.36 mg, 60-d release 17β-estradiol pellet (Innovative Research of America). BT-474M1 cells (5×10^6) in HBSS/Matrigel were injected s.c. into the right hind flank of each animal and then the animals were grouped into 10 treatment cohorts ($n = 4$) once the tumors reached a mean tumor volume of 200 to 250 mm^3. Each efficacy group was dosed with a combination of GDC-0941 (oral) daily and docetaxel (i.v.) weekly (20 and 10, 32 and 4.5, 32 and 15.5, 60 and 2.5, 60 and 10, 60 and 18, 88 and 4.5, 88 and 15.5, and 100 and 10 mg/kg, GDC-0941 and docetaxel, respectively). Vehicle mice were administered an oral dose of sterile-filtered, 13% EtOH. All animals were given a 24-h dosing holiday of GDC-0941 prior to the subsequent dose of docetaxel. Tumor volumes and animal weights were recorded biweekly and estrogen toxicity was monitored by bladder palpation. Dosing ended 21 d postimplantation and rebound tumor growth was monitored for an additional 10 d off drug treatment.

Statistical analysis for chemopotentiation. Contour plots for % inhibition were obtained by using the robust regression full quadratic model to obtain fitted values on the log(volume) scale, and then calculating % inhibition versus vehicle on the volume scale (23). *In vitro*, cells were treated with combinations of GDC-0941 (0, 15.625, 31.25, 62.5, 125, 500, 1,000, 2,000, 5,000, 10,000, and 20,000 nmol/L) and docetaxel (0, 0.2, 1.5625, 6.25, 12.5, 25, 50, and 100 nmol/L). *In vivo* cohorts included combinations of GDC-0941 (20, 32, 60, 88, and 100 mg/kg daily) and docetaxel (2.5, 4.5, 10, 15.5, and 18 mg/kg weekly).

Microarray hybridization and analysis. Cells were isolated from Matrigel in a PBS-EDTA buffer as mentioned above. RNA samples were harvested from the cells using an RNeasy kit (Qiagen) according to the manufacturer's instructions. Total RNA was isolated using the RNeasy RNA isolation kit from at least three independent cell cultures. Complementary RNA was synthesized and hybridized to Affymetrix U133 Plus 2.0 microarray chips. For hierarchical clustering, genes with a coefficient of variation ≥15% were selected. After standardizing genes by subtracting the gene mean and dividing by the gene SD, hierarchical clustering was done using average linkage and the Euclidean distance metric. For the comparison of heregulin-induced expression changes, *t*-statistics were calculated for the comparison of the vehicle- and heregulin-treated samples in the two-dimensional and three-dimensional lrECM environments, separately. For the analysis of gene sets differentially regulated in the two-dimensional and three-dimensional environments, two sets of *t*-statistics were calculated. *T*-statistics were calculated for the comparison of the two-dimensional plus heregulin condition versus the other three groups (two-dimensional – heregulin, three-dimensional – heregulin, and three-dimensional plus heregulin). Likewise, *t*-statistics were calculated for the comparison of the three-dimensional plus heregulin condition versus the other three groups (three-dimensional – heregulin, two-dimensional – heregulin, and two-dimensional plus heregulin). Gene set analysis was done for each of these ranked lists of *t*-statistics using GSEA 2.0 and the curated gene sets collection from MSigDB 2.5 (24).

Results

Cellular activity of GDC-0941 on breast cancer cell lines in three-dimensional culture. Medicinal chemistry efforts generated ATP-competitive thienopyrimidine inhibitors of the class I PI3K isoforms (p110α, β, δ, and γ) with excellent selectivity, potency, and physiochemical properties (ref. 19; Supplementary Fig. S1). GDC-0941 is equipotent against wild-type and oncogenic (E545K, H1047R) forms of PIK3CA enzyme (IC_{50} = 0.003 μmol/L) and the excellent enzyme activity translates into an effective reduction of phosphorylated levels of AKT in cells (MDA-MB-361 EC_{50} = 0.028 μmol/L). In comparison with PIK3CA inhibition, GDC-0941 is equipotent against PIK3CD, slightly weaker against PIK3CB (10-fold) and PIK3CG (25-fold), and highly selective against mammalian target of rapamycin (mTOR) and members of PI3K classes II, III, and IV (200-fold) enzymes (19). Hence, these cellular and biochemical properties make it possible to use GDC-0941 to characterize PI3K-directed pharmacologic intervention in breast cancer. We first investigated GDC-0941 responsiveness in a panel of breast cancer cell lines cultured in 3D lrECM in the presence or absence of 1 nmol/L heregulin (Fig. 1). Cell lines were classified according to their HER2, estrogen receptor and progesterone receptor status, histologic subtype, HER3 expression levels, 3D lrECM culture morphophology, and *PIK3CA* genotype (25–28). Common PIK3CA H1047R and E545K gain-of-function mutations were confirmed in 5 of 15 cell lines. In addition, three HER2/estrogen receptor–positive lines, BT474-M1, EFM192A, and ZR-75-30, contained atypical, and as yet uncharacterized, genetic aberrations within PIK3CA (K111N, C420R, and I139M, respectively). All cell lines express full-length PTEN protein as determined by immunoblotting with a PTEN-specific antibody (data not shown). As shown in Fig. 1, significant GDC-0941 single-agent activity (EC_{50} <1 μmol/L) was observed for 11 of 15 of cell lines as determined by measurement of cellular ATP concentration. Neither PIK3CA mutation nor hormone receptor status was a major determinant of GDC-0941 sensitivity in three-dimensional culture.

To better understand the role activated HER2/HER3 signaling may play in determining GDC-0941 responsiveness, the molecular and cellular impact of heregulin signaling was further investigated in 3D lrECM cultures. Given the correlation between acinar morphology and cell signaling in 3D lrECM conditions (28) and the described heregulin-induced phenotypic changes of mammary epithelial cells in 3D lrECM assays (8, 29), we hypothesized that heregulin treatment could lead to a distinct gene expression profile for BT-474M1, a prototypical HER2-amplified cell line, cultured in 3D lrECM. Encouragingly, unsupervised hierarchical clustering and statistical analysis of gene expression changes revealed that heregulin treatment in 3D lrECM culture exhibited significantly greater overall differential gene expression relative to cells grown on plastic with or without heregulin (Supplementary Fig. S2A and B). Functional classification of heregulin-induced genes revealed an enrichment of genes involved in hypoxia (a process known to be regulated by PI3K signaling) and cancer cell differentiation that was specific to three-dimensional culture conditions (Supplementary Fig. S2C). These findings were also confirmed by direct analysis of the hypoxia-induced signaling network and levels of hypoxia inducible factor-1α nuclear accumulation and vascular endothelial growth factor secretion were substantially decreased by PI3K inhibition in the context of 3D lrECM culture (Supplementary Fig. S2D). Based on this analysis of global gene expression, 3D lrECM culture is an appropriate model to study HER2/HER3 and PI3K pathway biology and combination therapy.

Increased resistance to GDC-0941 was observed for several cell lines following the addition of soluble heregulin to 3D lrECM cultures (Fig. 1A). Differential sensitivity was especially dramatic for MDA-MB-453, HCC1419, ZR-75-30, and T-47D, and heregulin treatment shifted the GDC-0941 EC_{50} by approximately 2-fold. These cells also exhibited the highest endogenous expression of HER3 that was most responsive to heregulin treatment, as determined by AKT phosphorylation

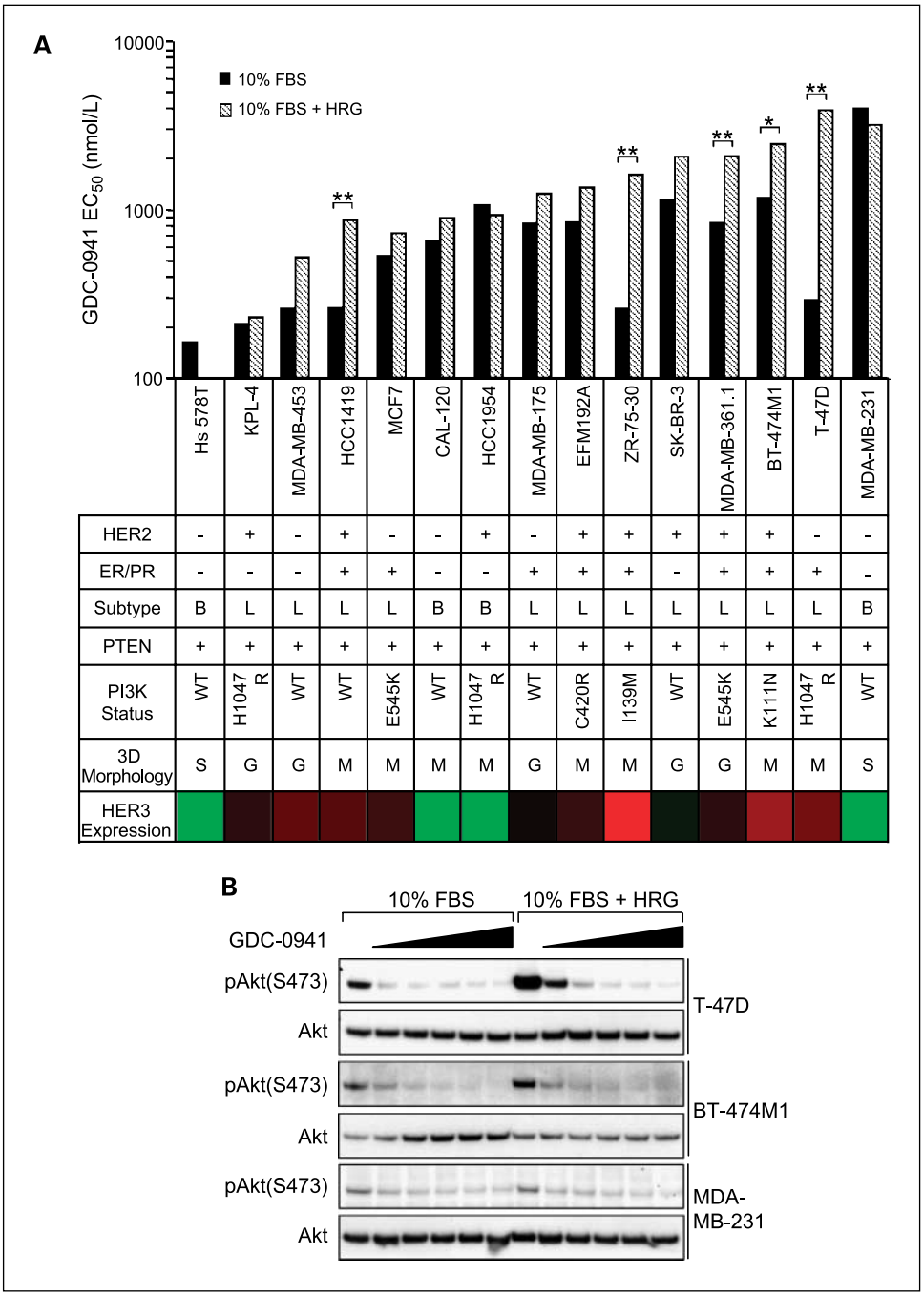

Fig. 1. *In vitro* response of breast cancer cell lines to PI3K inhibition in 3D lrECM culture. *A,* a panel of breast cancer cell lines was treated with 0 to 20 μmol/L GDC-0941 to determine the effects of PI3K inhibition in the presence and absence of 1 nmol/L heregulin (HRG) and to examine whether GDC-0941 sensitivity could be linked with heregulin response to HER2/estrogen receptor/progesterone receptor expression, clinical subtype, PI3K mutational status, PTEN expression, or colony morphology in 3D lrECM culture. M, mass (robust cell-cell adhesion); G, grape-like (poor cell-cell adhesion); S, stellate (elongated cell body with invasive processes). Cellular ATP levels were quantified with a bioluminescent assay and plotted against increasing concentrations of drug. Cell lines were seeded in 3D lrECM cultures on day 0, treated with GDC-0941 and/or 1 nmol/L heregulin on day 1, and assayed on day 4. *, $P < 0.05$; **, $P < 0.01$; Student's *t*-test. HER3 expression was determined by Affymetrix gene expression profiling and is color-coded according to the mean 202454.s.at probe intensity (*green*, low or absent; *black*, moderate; *red*, high). *B,* established 3D lrECM cultures of BT474-M1, T-47D, and MDA-MB-231 cells were treated with increasing concentrations of GDC-0941 (0, 100, 250, 500, 1,000, and 2,000 nmol/L) in the presence or absence of 1 nmol/L HRG for 24 h. Pathway inhibition was assessed by immunoblotting for Akt-Ser473 phosphorylation.

(Fig. 1B). MDA-MB-175 was also responsive to exogenous heregulin in our assays despite having constitutive heregulin autocrine signaling (30). In comparison, neither GDC-0941 sensitivity nor Akt phosphorylation of basal breast cancer cell lines (Hs 578T, Cal-120, HCC1954 and MDA-MB-231) was affected by heregulin signaling (Fig. 1B). Taken together, heregulin-dependent signaling is sufficient to bypass single-agent PI3K inhibition in a subset of HER2-amplified and luminal breast cancer cells.

Enhanced effect of GDC-0941, trastuzumab, and pertuzumab combination on growth and morphogenesis of BT-474M1 acini. To extend our analysis of PI3K inhibition in breast cancer, GDC-0941 combination with trastuzumab and pertuzumab was evaluated using BT-474M1 cells in 3D lrECM culture. Therapeutic antibodies were used at saturating concentrations of 20 μg/mL and 25 μg/mL for trastuzumab and pertuzumab, respectively. The minimum GDC-0941 concentration for effective target inhibition was determined by assessment of phosphorylated AKT, cell viability, and acinar phenotype over a 9-day treatment period. GDC-0941 of 250 nmol/L potently inhibited PI3K downstream signaling over a 24-hour time period and this concentration was selected for 3D lrECM combination assays (Fig. 2A). As a single agent, GDC-0941 treatment reduced acinar size in normal media but

had a limited effect on heregulin-induced morphogenesis (Fig. 2B and C). Consistent with prior observations (8), pertuzumab effectively blocked acinar morphogenesis without impacting overall growth in the presence of heregulin. Growth attenuation was also not observed following combined treatment of trastuzumab and pertuzumab in heregulin-containing 3D lrECM culture conditions. Strikingly, the triple combination of GDC-0941, trastuzumab, and pertuzumab synergistically reduced acinar size and morphogenesis in both heregulin-supplemented and standard media ($P < 0.0001$,

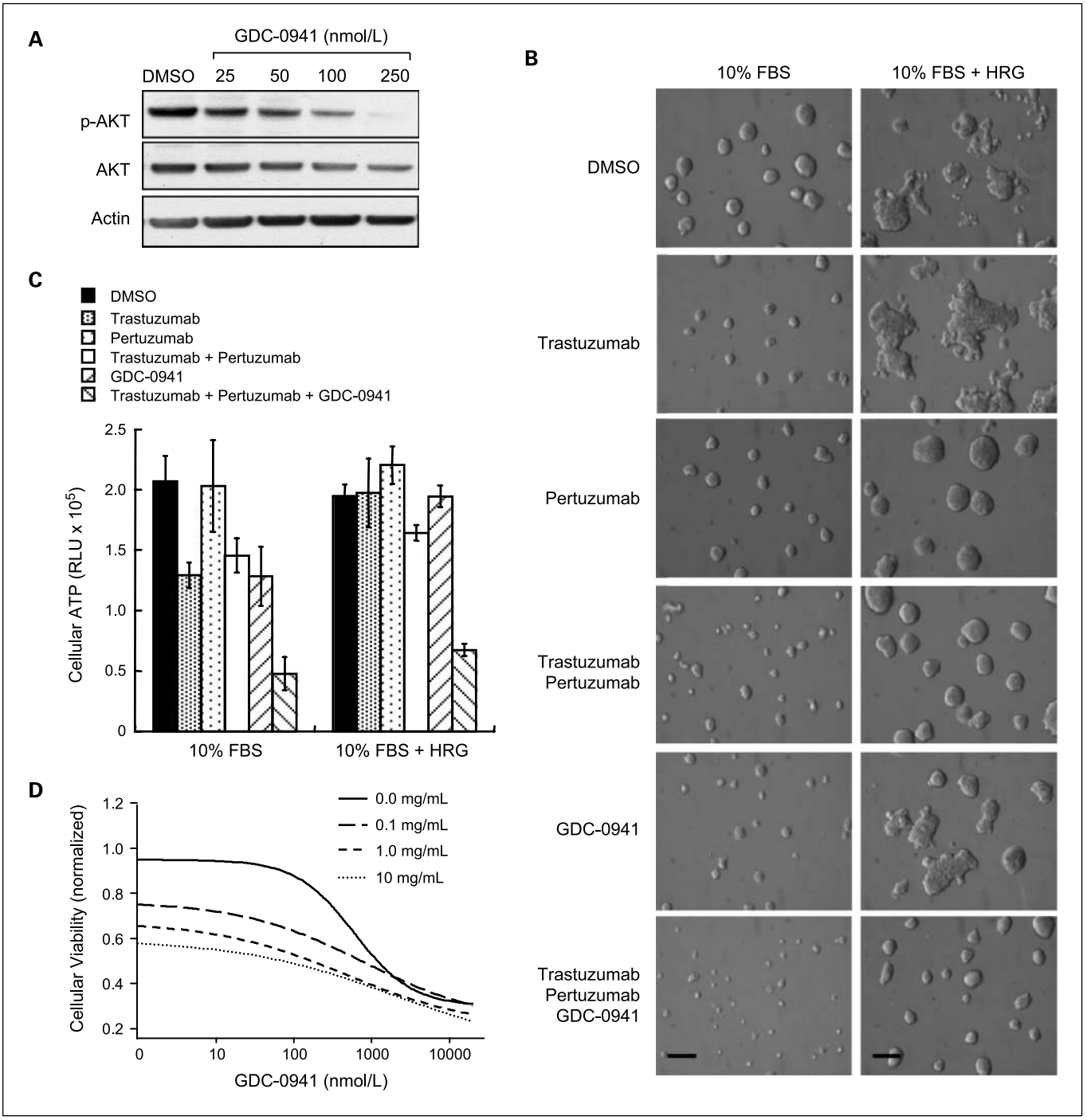

Fig. 2. Enhanced effect of the GDC-0941, trastuzumab, and pertuzumab combination on growth and morphogenesis of BT-474M1 acini. BT-474M1 cells in 3D lrECM culture were tested for their sensitivity to inhibitors. *A,* cells were treated with GDC-0941 for 24 h, lysed, and immunoblotted for phosphorylated AKT. Equal loading was confirmed by detection of total AKT and β-actin protein levels. *B,* a range of drug effects can be distinguished in 3D lrECM culture through variations in cellular morphology. Phase contrast images show representative phenotypes of cells treated with 20 μg/mL trastuzumab, 25 μg/mL pertuzumab, 250 nmol/L GDC-0941 as single agent or in combination after 9 d in culture. Scale bar, 10 μmol/L. *C,* quantified ATP levels were used to confirm the efficacy of drug combinations in 3D lrECM cultures. Error bars, mean ± SD. *D,* cells were treated with equal concentrations of trastuzumab and pertuzumab (0-10 μg/mL) and increasing doses of GDC-0941 for a total of 3 d in 3D lrECM culture with normal media. Cell viability was recorded and standardized against the mean of 9 independent control samples.

Dunnett's *t*-test; Fig. 2C). The activity of GDC-0941, trastuzumab, and pertuzumab combination exceeded that of GDC-0941 pairing with either trastuzumab or pertuzumab individually (Supplementary Fig. S3). Inhibition of BT-474M1 acinar growth was also evident from GDC-0941 dose ranging with trastuzumab and pertuzumab at increasing concentrations in normal media (Fig. 2D). Slope parameters from a 4-parameter logistic curve were 1.17, 0.55, 0.52, and 0.44 for 0, 0.1, 1, and 10 μg/mL of the HER2 antibodies, respectively. Despite the observed morphologic changes, relocalization of common cell polarity markers (p85 PI3K, PIP3, GM130 and α6 integrin) was not observed by immunofluorescence imaging of BT-474M1 acini following administration of PI3K and HER2 inhibitors (data not shown). This suggests that the inhibition of additional pathways may still be required for a full phenotypic reversion of BT-474M1 acini (31, 32). In summary, BT-474M1 growth and morphology in 3D lrECM culture can be used to characterize the activity of therapeutic agents, and our data suggest that combined administration of GDC-0941, trastuzumab, and pertuzumab may provide improved efficacy for HER2-amplified breast cancer.

Disruption of PI3K-AKT and RAF-MEK effector signaling by GDC-0941, trastuzumab, and pertuzumab treatment. We next investigated the molecular mechanism of action for GDC-0941, trastuzmab, and pertuzumab in order to better understand the signaling pathways that regulate acinar growth and morphology of HER2-amplified breast cancer cells. Using BT-474M1 acini in 3D lrECM culture, administration of GDC-0941, trastuzumab, and pertuzumab for 24 hours profoundly reduced basal activity of RAF and PI3K pathways as measured by antibodies specific to phosphorylated MEK (Ser217/221) and AKT (Ser473), respectively (Fig. 3). As a control, no differences were noted for total MEK, AKT, or β-actin protein levels. The GDC-0941, trastuzumab, and pertuzumab combination resulted in significant, sustained inhibition of MEK and AKT phosphorylation in the presence of heregulin (*lane 12*). Greater attenuation of phosphorylation was observed for AKT than for MEK under these conditions. In comparison with the triple combination, trastuzumab and pertuzumab alone were not sufficient to prevent either heregulin-induced signaling (*lane 10*) or proliferation (Fig. 2C). Consistent with previous reports, a compensatory increase in HER3 phosphorylation was also observed following PI3K inhibition (*lane 11*; ref. 33). Taken together, the extent of pharmacodynamic modulation of MEK and AKT pathways correlated well with changes in acinar growth and phenotype resulting from inhibition of HER2/HER3 and PI3K catalytic activity in HER2-amplified cells.

Maximum combinatorial efficacy of GDC-0941 with inhibition of HER2-HER3 heterodimer activity. Lapatinib is an epidermal growth factor receptor and HER2 tyrosine kinase inhibitor that is approved for breast cancer (34). Because inhibition of HER2 by lapatinib also leads to a reduction in HER3 transphosphorylation in biochemical assays (35), this inhibitor was benchmarked against trastuzumab and pertuzumab to further examine the functional role of HER2/HER3 in 3D lrECM combination assays. Administration of 200 nmol/L lapatinib resulted in significant inhibition of epidermal growth factor receptor, HER2, HER3, and Akt phosphorylation in normal 3D lrECM culture conditions (Fig. 4A) as well as in the presence of exogenous heregulin (Supplementary Fig. S4). At this concentration, lapatinib treatment did not affect cell proliferation in the presence of heregulin, and growth inhibition was significantly greater for triple combination of GDC-0941, trastuzumab, and pertuzumab than for GDC-0941 plus lapatinib ($P < 0.0001$, Dunnett's *t*-test; Fig. 4B). Given that acini treated with GDC-0941, trastuzumab, and pertuzumab displayed a significant qualitative decrease in morphogenesis (Fig. 4C), high-throughput, quantitative methods were developed to more accurately assess 3D lrECM phenotypes as a measure of drug efficacy. Phase-contrast images of BT-474M1 acini were analyzed for total area and shape. The shape factor algorithm is defined as $(4\pi*\text{Area})/(\text{Perimeter}^2)$ and yields values ranging from 0 (flat line) to 1 (perfect circle). By this analysis, lapatinib was less efficacious in combination with GDC-0941 than was trastuzumab, pertuzumab, and GDC-0941 ($P = 0.013$, area; $P = 0.0095$, shape factor; Fig. 4D). Also, the effect of the GDC-0941, trastuzumab, and pertuzumab combination on acinar size and morphology was shown to be additive by Bliss analysis (data not shown). Taken together, these results provide substantial support for the current view that HER2-HER3 catalytic activity is important for driving tumor cell proliferation and suggests a unique mechanism of action for GDC-0941 combination with trastuzumab and pertuzumab compared with small molecule HER2 inhibitors, such as lapatinib.

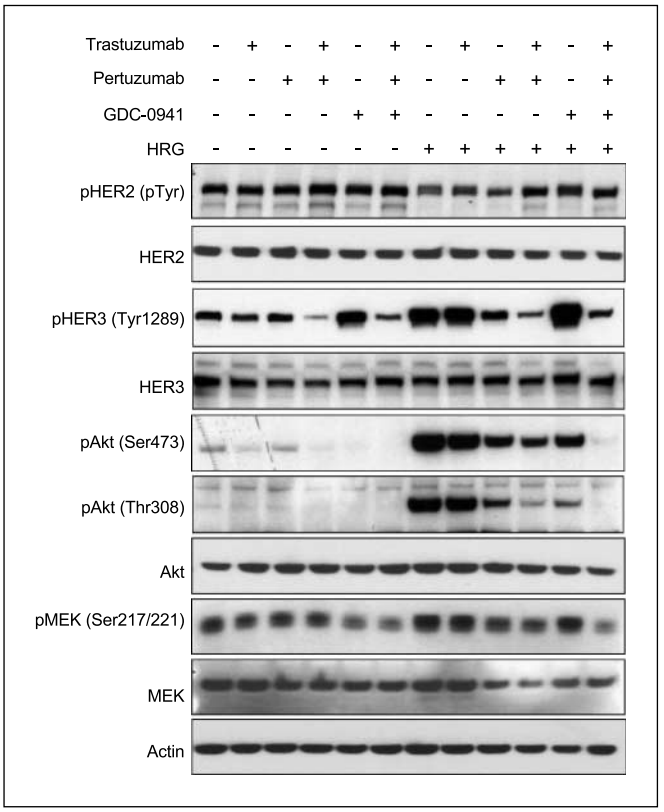

Fig. 3. The PI3K-AKT and RAF-MEK signaling pathways are disrupted in BT-474M1 acini treated with GDC-0941, trastuzumab, and pertuzumab. BT-474M1 cell lysates were collected and analyzed for phosphorylation of downstream biomarkers. Changes in downstream signaling were monitored by detecting phosphorylated proteins at well-characterized activation site residues: HER2 (total tyrosine), HER3 (Tyr1289), Akt (Thr308 and Ser473), and MEK (Ser217/221). Total protein and β-actin were used as loading controls.

GDC-0941, trastuzumab, and pertuzumab combination is efficacious in a panel of HER2-amplified breast cancer cell lines. To extend our observations for GDC-0941 combination

therapy, GDC-0941, trastuzumab, and pertuzumab were tested using additional cell lines to reflect common genetic heterogeneity and varying trastuzumab response in HER2-amplified breast cancer. As shown in Fig. 5, PI3K inhibitor treatment showed good single-agent potency under normal culture conditions and was effective in EFM192A and HCC1954 cells

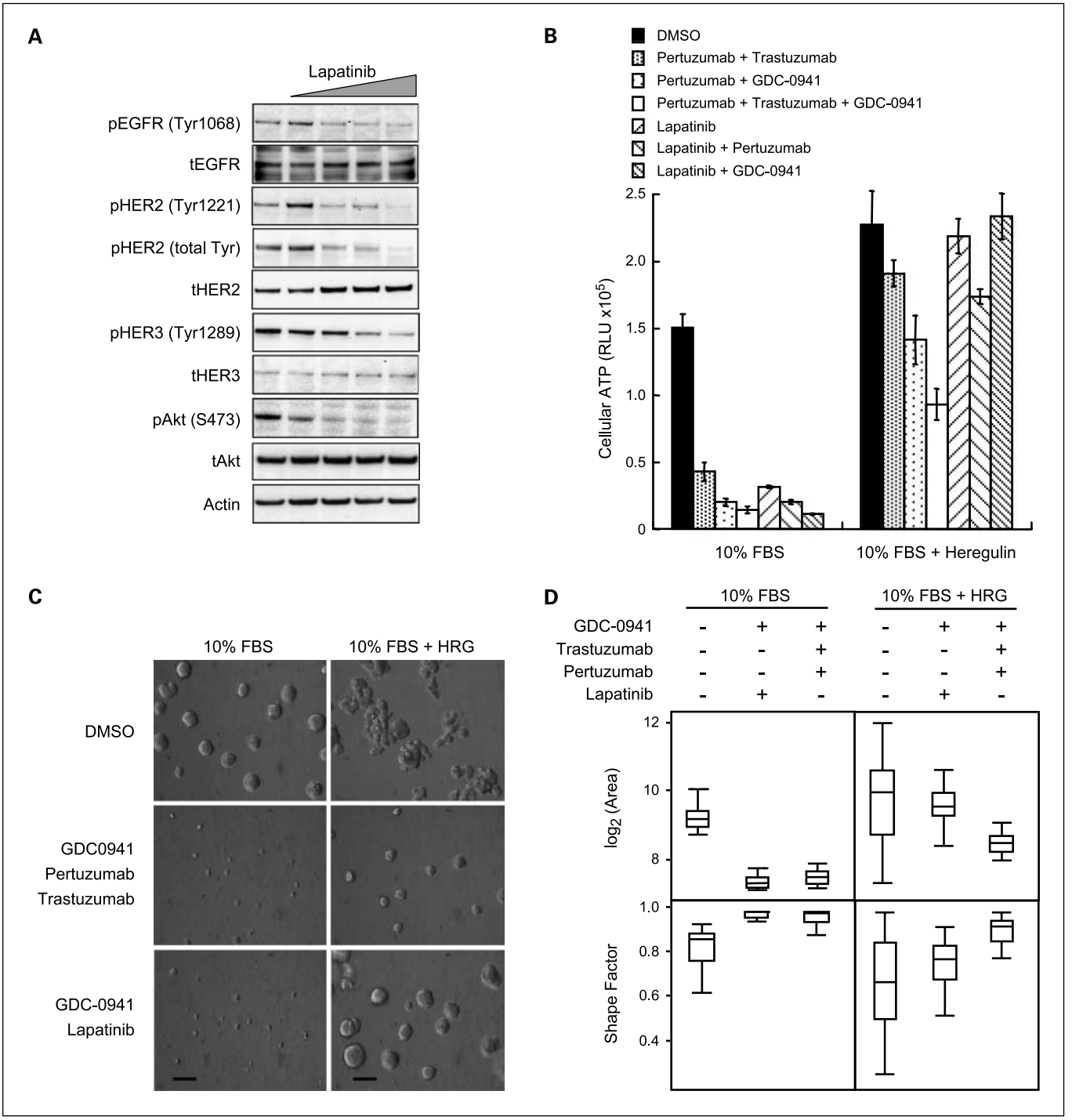

Fig. 4. 3D lrECM culture comparison of GDC-0941 combination with either lapatinib or HER2-specific antibodies. *A,* a working concentration of lapatinib was selected by titrating the compound in 3D lrECM cell culture. Drug efficacy was determined by detecting epidermal growth factor receptor, HER2, HER3, and Akt phosphorylation levels in cells pretreated with lapatinib at 0, 50, 100, 200, and 300 nmol/L concentrations for 7 d. Phosphorylated protein levels were normalized to total proteins and β-actin. *B,* combinations of GDC-0941, trastuzumab, pertuzumab, and lapatinib were administered to BT-474M1 cells in 3D lrECM culture as indicated. The overall effectiveness of drug combinations on inhibition of cell proliferation was quantified by cellular ATP measurement. Error bars, mean ± SD. Treatment with the GDC-0941, trastuzumab, and pertuzumab combination resulted in the greatest inhibition of acinar growth compared with all other treatment groups ($P < 0.0001$, Dunnett's *t*-test). *C,* differences in drug mechanism are illustrated by variations in cell morphology. Scale bar, 10 μmol/L. *D,* the efficacy of drug combinations was assessed by a mathematical distribution of acinar size (area) and shape (shape factor). Data are plotted as the mean (*horizontal line*), middle 50% of data (*box*), and 95% confidence interval (*lines*). Pair-wise comparisons were done by Student's *t*-test. The GDC-0941, trastuzumab, and pertuzumab combination resulted in significant morphology changes in both the presence or absence of heregulin in the culture media ($P < 0.0001$, area or shape factor). GDC-0941 and lapatinib combination resulted in significant morphology changes in normal culture media ($P < 0.0001$, area or shape factor) and in media containing heregulin ($P = 0.035$, area; $P = 0.017$, shape factor).

in the presence of heregulin. However, the strongest inhibition of proliferation for all cell lines in 3D lrECM culture was noted for the GDC-0941, trastuzumab, and pertuzumab combination in normal media and media supplemented with heregulin. HCC1419 cell proliferation was moderately reduced when HER2 signaling was perturbed using trastuzumab or pertuzumab together but not as single agents (Fig. 5A). In comparison, HCC1419 proliferation was dramatically inhibited upon treatment with GDC-0941, trastuzumab, and pertuzumab in combination. The response of EFM192A cells to inhibitors was not altered by heregulin addition and following 9 days a 90% decrease in acinar growth was observed for GDC-0941, trastuzumab, and pertuzumab relative to control (Fig. 5B). HCC1954 cells are classified in the basal-like subtype of HER2-amplified breast cancer. Because this subtype has been associated with poor prognosis in the clinic (36) it is encouraging that GDC-0941 treatment as a single agent and in combination with trastuzumab and pertuzumab showed potent efficacy in 3D lrECM assays (Fig. 5C). In addition, the sensitivity profile to these therapeutic agents of an additional cell line of the luminal HER2-amplified subtype, SK-BR-3, was comparable with that of BT-474M1 (data not shown). Taken together, we show that the efficacy of GDC-0941, trastuzumab, and pertuzumab combination therapy in 3D lrECM culture is a general phenomenon and not a peculiarity of one cell line. Although sensitivity to either HER2/HER3 or PI3K inhibition is well correlated with HER2 amplification in breast tumor cell lines, only the GDC-0941, trastuzumab, and pertuzumab combination was consistently effective in preventing tumor cell growth in the context of HER3 activation by heregulin.

***GDC-0941 potentiates docetaxel-induced growth inhibition* in vitro *and* in vivo.** Several mechanisms have been proposed for the action of anti-HER2 therapies, including interruption of the PI3K pathway to enhance sensitivity to taxanes, a family of cytotoxic drugs that are commonly used in combination with trastuzumab for treatment of HER2-amplified breast cancer (14, 37, 38). Therefore, we used GDC-0941 to directly investigate the impact of PI3K inhibition on sensitivity of HER2-amplified cells to docetaxel. Extensive dose ranging was done for both agents in 3D lrECM culture and combinatorial growth inhibition was observed for BT-474M1 cells (Supplementary Fig. S5A). For instance, whereas 85% inhibition of tumor cell proliferation was achieved using either 2,000 nmol/L GDC-0941 or 30 nmol/L docetaxel when administered as single agents, an equivalent cellular response resulted from lower doses of both agents in combination (250 nmol/L GDC-0941 and 7 nmol/L docetaxel). Cellular activity in 3D lrECM culture also correlated well with *in vivo* efficacy of GDC-0941 and docetaxel (Supplementary Fig. S5B). Taken together, GDC-0941 shows combinatorial efficacy with targeted therapeutics and standard-of-care chemotherapeutic agents that are commonly used in the clinical management of HER2-amplified breast cancer. As previously shown for anticancer chemotherapeutic agents, the behavior of tumor cells grown in monolayer or suspension can differ significantly from the three-dimensional culture environment (39, 40). Hence, 3D lrECM models may have better predictive value for determining preclinical efficacy and can be used to select tumor cell lines for further *in vivo* characterization.

Discussion

GDC-0941 is an orally bioavailable PI3K inhibitor that exhibits robust activity and provides a selective tool to dissect the role of class I PI3K in breast cancer biology. We utilized 3D lrECM culture as a preclinical model to examine PI3K-directed pharmacologic intervention in HER2-amplified breast cancer and dissect the cellular and signaling responses to various combinations of GDC-0941 and HER2/HER3 pathway inhibitors. We show that PI3K inhibition acts in concert with trastuzumab, pertuzumab (Figs. 2 and 5), and docetaxel (Supplementary Fig. S5) to decrease the growth and morphogenesis of HER2-amplified tumor cells. Accordingly, HER2 and PI3K inhibition also resulted in synergistic modulation of effector signaling as determined by AKT and MEK phosphorylation (Fig. 3). These results provide strong evidence that the

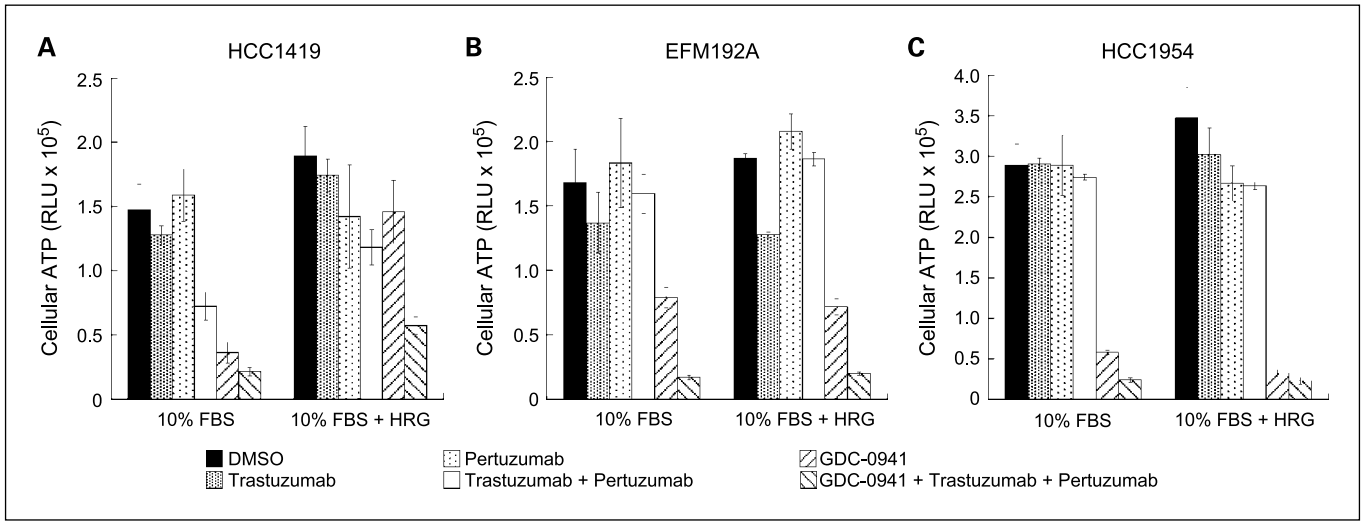

Fig. 5. GDC-0941, trastuzumab, and pertuzumab combination in a panel of HER2-amplified breast cancer cell lines. HER2-amplified cell lines were examined for their overall response to combination therapy. *A,* HCC1419, (*B*) EFM192A, and (*C*) HCC1954 cells were cultured in 3D lrECM with or without 1 nmol/L heregulin (HRG). Each cell line was treated with 20 μg/mL trastuzumab, 25 μg/mL pertuzumab, and GDC-0941 (250 nmol/L GDC-0941 used for EFM192A and HCC1419; 1 μmol/L GDC-0941 used for HCC1954), and response was determined by measuring cellular ATP levels. Error bars, mean ± SD.

addition of PI3K inhibitor to HER2-directed treatment could augment clinical benefit in breast cancer patients.

It is encouraging that PI3K inhibitors may have broad utility across several breast cancer subtypes (Fig. 1). However, heregulin-induced signaling was associated with differential sensitivity to either PI3K or HER2 pathway therapy (Figs. 1 and 2). HER2 inhibitors with differing molecular mechanisms were compared for combinatorial activity with PI3K inhibition (Fig. 4), and the potent efficacy of GDC-0941 with trastuzumab and pertuzumab, which disrupts the HER2/HER3 complex, is consistent with HER3 playing a major role in HER2-amplified breast cancer (8). These results also have clear implications in light of the autocrine expression of heregulin in breast tumors (41–43) and metastatic potential of cells expressing HER3 ligands (44). Taken together, *a priori* analysis of tumor biopsies for HER3 activation or downstream signaling may help stratify patients likely to benefit from combination therapy.

Our experiments further illustrate how 3D lrECM models can be applied to pharmaceutical drug development. We utilized a three-dimensional culture platform to explore therapeutic combinations of several clinically relevant inhibitors and examined the molecular mechanisms that underlie the efficacy of these molecules. It is noteworthy that enhanced activity of the trastuzumab, pertuzumab, and laptinib combination was also observed in heregulin-stimulated 3D lrECM cultures (Supplementary Fig. S6), suggesting further strategies for combining HER2 inhibitors for the treatment of HER2-positive breast cancer (45). In the course of this project, several advancements were made to traditional three-dimensional culture methods, including automated, binary analysis to quantify changes in acinar structure (Fig. 4) and a response surface experimental design to better conduct combination studies and correlate three-dimensional cell culture and *in vivo* efficacy (Supplementary Fig. S5). Our results show that three-dimensional culture models can be used effectively in drug development and suggest that targeting parallel pathways in HER2/HER3 and PI3K signaling is a viable strategy for the treatment of breast cancer.

Disclosure of Potential Conflicts of Interest

All authors are employees of Genentech, Inc.

Acknowledgments

We thank Howard Stern, Deepak Sampath, Gabriele Schaefer, Robert Akita, Matt Brauer, and Alex Andrus for helpful discussions, and Ken Jung, Zora Modrusan, and the microarray core lab for technical support.

References

1. Sugimoto Y, Whitman M, Cantley LC, Erikson RL. Evidence that the Rous sarcoma virus transforming gene product phosphorylates phosphatidylinositol and diacylglycerol. Proc Natl Acad Sci U S A 1984;81:2117–21.
2. Engelman JA, Luo J, Cantley LC. The evolution of phosphatidylinositol 3-kinases as regulators of growth and metabolism. Nat Rev 2006;7:606–19.
3. Bader AG, Kang S, Zhao L, Vogt PK. Oncogenic PI3K deregulates transcription and translation. Nat Rev Cancer 2005;5:921–9.
4. Samuels Y, Wang Z, Bardelli A, et al. High frequency of mutations of the PIK3CA gene in human cancers. Science 2004;304:554.
5. Wishart MJ, Dixon JE. PTEN and myotubularin phosphatases: from 3-phosphoinositide dephosphorylation to disease. Trends Cell Biol 2002;12:579–85.
6. Marone R, Cmiljanovic V, Giese B, Wymann MP. Targeting phosphoinositide 3-kinase: moving towards therapy. Biochim Biophys Acta 2008;1784:159–85.
7. Yarden Y, Sliwkowski MX. Untangling the ErbB signalling network. Nat Rev Mol Cell Biol 2001;2:127–37.
8. Lee-Hoeflich ST, Crocker L, Yao E, et al. A central role for HER3 in HER2-amplified breast cancer: implications for targeted therapy. Cancer Res 2008;68:5878–87.
9. Yakes FM, Chinratanalab W, Ritter CA, King W, Seelig S, Arteaga CL. Herceptin-induced inhibition of phosphatidylinositol-3 kinase and Akt Is required for antibody-mediated effects on p27, cyclin D1, and antitumor action. Cancer Res 2002;62:4132–41.
10. Hsieh AC, Moasser MM. Targeting HER proteins in cancer therapy and the role of the non-target HER3. Br J Cancer 2007;97:453–7.
11. Fedi P, Pierce JH, di Fiore PP, Kraus MH. Efficient coupling with phosphatidylinositol 3-kinase, but not phospholipase C γ or GTPase-activating protein, distinguishes ErbB-3 signaling from that of other ErbB/EGFR family members. Mol Cell Biol 1994;14:492–500.
12. Motoyama AB, Hynes NE, Lane HA. The efficacy of ErbB receptor-targeted anticancer therapeutics is influenced by the availability of epidermal growth factor-related peptides. Cancer Res 2002;62:3151–8.
13. Berns K, Horlings HM, Hennessy BT, et al. A functional genetic approach identifies the PI3K pathway as a major determinant of trastuzumab resistance in breast cancer. Cancer Cell 2007;12:395–402.
14. Nagata Y, Lan KH, Zhou X, et al. PTEN activation contributes to tumor inhibition by trastuzumab, and loss of PTEN predicts trastuzumab resistance in patients. Cancer Cell 2004;6:117–27.
15. Debnath J, Brugge JS. Modelling glandular epithelial cancers in three-dimensional cultures. Nat Rev Cancer 2005;5:675–88.
16. Nelson CM, Bissell MJ. Of extracellular matrix, scaffolds, and signaling: tissue architecture regulates development, homeostasis, and cancer. Ann Rev Cell Dev Biol 2006;22:287–309.
17. Yamada KM, Cukierman E. Modeling tissue morphogenesis and cancer in 3D. Cell 2007;130:601–10.
18. Lee GY, Kenny PA, Lee EH, Bissell MJ. Three-dimensional culture models of normal and malignant breast epithelial cells. Nat Methods 2007;4:359–65.
19. Folkes AJ, Ahmadi K, Alderton WK, et al. The Identification of 2-(1H-Indazol-4-yl)-6-(4-methanesulfonyl-piperazin-1-ylmethyl)-4-morpholin-4-yl-thieno[3,2-d]pyrimidine (GDC-0941) as a potent, selective, orally bioavailable inhibitor of class I PI3 kinase for the treatment of cancer. J Med Chem 2008;51:5522–32.
20. Agus DB, Akita RW, Fox WD, et al. Targeting ligand-activated ErbB2 signaling inhibits breast and prostate tumor growth. Cancer Cell 2002;2:127–37.
21. Gelmon KA, Fumoleau P, Verma S, et al. Results of a phase II trial of trastuzumab and pertuzumab in patients with HER2-positive metastatic breast cancer who had progressed during trastuzumab therapy. J Clin Oncol 2008;26.
22. Holmes WE, Sliwkowski MX, Akita RW, et al. Identification of heregulin, a specific activator of p185erbB2. Science New York NY 1992;256:1205–10.
23. Anton H. Calculus: a new horizon. 6th Ed. New York: Wiley; 1984. p. 870–2.
24. Subramanian A, Tamayo P, Mootha VK, et al. Gene set enrichment analysis: a knowledge-based approach for interpreting genome-wide expression profiles. Proc Natl Acad Sci U S A 2005;102:15545–50.
25. Forbes S, Clements J, Dawson E, et al. Cosmic 2005. Br J Cancer 2006;94:318–22.
26. Kurebayashi J, Otsuki T, Tang CK, et al. Isolation and characterization of a new human breast cancer cell line, KPL-4, expressing the Erb B family receptors and interleukin-6. Br J Cancer 1999;79:707–17.
27. Neve RM, Chin K, Fridlyand J, et al. A collection of breast cancer cell lines for the study of functionally distinct cancer subtypes. Cancer Cell 2006;10:515–27.
28. Kenny PA, Lee GY, Myers CA, et al. The morphologies of breast cancer cell lines in three-dimensional assays correlate with their profiles of gene expression. Mol Oncol 2007;1:84–96.
29. Sternlicht MD, Sunnarborg SW, Kouros-Mehr H, Yu Y, Lee DC, Werb Z. Mammary ductal morphogenesis requires paracrine activation of stromal EGFR via ADAM17-dependent shedding of epithelial amphiregulin. Development 2005;132:3923–33.
30. Schaefer G, Fitzpatrick VD, Sliwkowski MX. γ-Heregulin: a novel heregulin isoform that is an autocrine growth factor for the human breast cancer cell line, MDA-MB-175. Oncogene 1997;15:1385–94.
31. Wang F, Hansen RK, Radisky D, et al. Phenotypic reversion or death of cancer cells by altering signaling pathways in three-dimensional contexts. J Natl Cancer Inst 2002;94:1494–503.
32. Liu H, Radisky DC, Wang F, Bissell MJ. Polarity and proliferation are controlled by distinct signaling pathways downstream of PI3-kinase in breast epithelial tumor cells. J Cell Biol 2004;164:603–12.
33. Sergina NV, Rausch M, Wang D, et al. Escape from HER-family tyrosine kinase inhibitor therapy by the kinase-inactive HER3. Nature 2007;445:437–41.
34. Moasser MM. Targeting the function of the HER2 oncogene in human cancer therapeutics. Oncogene 2007;26:6577–92.
35. Xia W, Liu LH, Ho P, Spector NL. Truncated ErbB2 receptor (p95ErbB2) is regulated by heregulin through heterodimer formation with ErbB3 yet

remains sensitive to the dual EGFR/ErbB2 kinase inhibitor GW572016. Oncogene 2004;23:646–53.

36. Liu H, Fan Q, Zhang Z, Li X, Yu H, Meng F. Basal-HER2 phenotype shows poorer survival than basal-like phenotype in hormone receptor-negative invasive breast cancers. Human Pathology 2008;39:167–74.

37. Pegram MD, Konecny GE, O'Callaghan C, Beryt M, Pietras R, Slamon DJ. Rational combinations of trastuzumab with chemotherapeutic drugs used in the treatment of breast cancer. J Natl Cancer Inst 2004;96:739–49.

38. Azambuja E, Durbecq V, Rosa DD, et al. HER-2 overexpression/amplification and its interaction with taxane-based therapy in breast cancer. Ann Oncol 2008;19:223–32.

39. Debnath J, Mills KR, Collins NL, Reginato MJ, Muthuswamy SK, Brugge JS. The role of apoptosis in creating and maintaining luminal space within normal and oncogene-expressing mammary acini. Cell 2002;111:29–40.

40. Weaver VM, Lelievre S, Lakins JN, et al. β 4 integrin-dependent formation of polarized three-dimensional architecture confers resistance to apoptosis in normal and malignant mammary epithelium. Cancer Cell 2002;2:205–16.

41. Huang HE, Chin SF, Ginestier C, et al. A recurrent chromosome breakpoint in breast cancer at the NRG1/neuregulin 1/heregulin gene. Cancer Res 2004;64:6840–4.

42. Li Q, Ahmed S, Loeb JA. Development of an autocrine neuregulin signaling loop with malignant transformation of human breast epithelial cells. Cancer Res 2004;64:7078–85.

43. Montero JC, Rodriguez-Barrueco R, Ocana A, Diaz-Rodriguez E, Esparis-Ogando A, Pandiella A. Neuregulins and cancer. Clin Cancer Res 2008;14:3237–41.

44. Meiners S, Brinkmann V, Naundorf H, Birchmeier W. Role of morphogenetic factors in metastasis of mammary carcinoma cells. Oncogene 1998;16:9–20.

45. O'Shaughnessy J, Blackwell KL, Burstein H, et al. A randomized study of lapatinib alone or in combination with trastuzumab in heavily pretreated HER2+ metastatic breast cancer progressing on trastuzumab therapy. ASCO Meeting Abstracts 2008;26:1015.